Journal of Experimental Botany, Vol. 70, No. 21 pp. 6337–6348, 2019
doi:10.1093/jxb/erz359 Advance Access Publication August 6, 2019
This paper is available online free of all access charges (see https://academic.oup.com/jxb/pages/openaccess for further details)

RESEARCH PAPER

Histone acetyltransferase GCN5-mediated regulation of long non-coding RNA *At4* contributes to phosphate starvation response in Arabidopsis

Tianya Wang[1,2,3,*], Jiewen Xing[2,3,*], Zhenshan Liu[2,3], Mei Zheng[2,3], Yingyin Yao[2,3], Zhaorong Hu[2,3], Huiru Peng[2,3], Mingming Xin[2,3], Daoxiu Zhou[4] and Zhongfu Ni[2,3,†]

[1] Key Laboratory of Molecular Epigenetics of the Ministry of Education (MOE), Northeast Normal University, Changchun, 130024, China
[2] State Key Laboratory of Agrobiotechnology, Key Laboratory of Crop Heterosis and Utilization (MOE), Key Laboratory of Crop Genetic Improvement (Beijing Municipality), China Agricultural University, Beijing, 100193, China
[3] College of Agronomy and Biotechnology, China Agricultural University, Yuanmingyuan Xi Road No. 2, Haidian District, Beijing, 100193, China
[4] Institut of Plant Science Paris-Saclay, Université Paris sud, 91405 Orsay, France

* These authors contributed equally to this work.
† Correspondence: nizf@cau.edu.cn

Received 21 March 2019; Editorial decision 19 July 2019; Accepted 19 July 2019

Editor: Ramanjulu Sunkar, Oklahoma State University, USA

Abstract

Phosphate availability is becoming a limiting environmental factor that inhibits plant growth and development. Here, we demonstrated that mutation of the histone acetyltransferase GCN5 impaired phosphate starvation responses (PSRs) in Arabidopsis. Transcriptome analysis revealed that 888 GCN5-regulated candidate genes were potentially involved in responding to phosphate starvation. ChIP assay indicated that four genes, including a long non-coding RNA (lncRNA) *At4*, are direct targets of GCN5 in PSR regulation. In addition, GCN5-mediated H3K9/14 acetylation of *At4* determined dynamic *At4* expression. Consistent with the function of *At4* in phosphate distribution, mutation of GCN5 impaired phosphate accumulation between shoots and roots under phosphate deficiency condition, whereas constitutive expression of *At4* in *gcn5* mutants partially restored phosphate relocation. Further evidence proved that GCN5 regulation of *At4* influenced the miRNA miR399 and its target *PHO2* mRNA level. Taken together, we propose that GCN5-mediated histone acetylation plays a crucial role in PSR regulation via the *At4–miR399–PHO2* pathway and provides a new epigenetic mechanism for the regulation of lncRNA in plants.

Keywords: *Arabidopsis thaliana*, *At4*, GCN5, histone acetylation, lncRNA, phosphate starvation response.

Introduction

Phosphorus is an essential macronutrient for plant metabolic processes, including energy metabolism, synthesis of nucleic acids and membranes, photosynthesis, respiration, nitrogen fixation, and enzyme regulation (Raghothama, 1999). Phosphate (Pi) deficiency is a limiting factor for plant growth and productivity in 40% of the world's arable soils (Vance,

Abbreviations: FDR, false discovery rate; GCN5, general control non-repressed protein5; GO, Gene Ontology;HAT, histone acetyltransferase; HDAC, histone deacetylase;lncRNA, long non-coding RNA; PSR, phosphate starvation response; RSA, root system architecture.

2001). To cope with this, plants have evolved regulatory mechanisms to maintain phosphorus homeostasis by improving Pi uptake, translocation, remobilization, and efficiency of use (Lin *et al.*, 2009; Rouached *et al.*, 2010; Chiou and Lin, 2011; Liang *et al.*, 2014; Wang *et al.*, 2018). Under Pi-limited conditions, plants usually exhibit modified RSA (root system architecture), including reduced primary root, increased number and density of root hairs, and the secretion of phosphatases and organic acids (Lambers *et al.*, 2003, 2006; Fang *et al.*, 2009; Yang and Finnegan, 2010; Xu *et al.*, 2019).

Non-coding RNA is one of the key regulators involved in the phosphate starvation response (PSR) network (Rouached *et al.*, 2010; Yang and Finnegan, 2010). The expression of the miRNA *miR399* is strongly induced upon Pi starvation, especially in vascular tissues of the shoot. Mature *miR399* is then translocated to roots and binds to the 5'-untranslated region (UTR) of its target *PHOSPHATE2* (*PHO2*) transcripts, leading to the degradation of *PHO2* mRNA (Bari *et al.*, 2006; Lin *et al.*, 2008; Du *et al.*, 2018). PHO2, an E2 ubiquitin-conjugating enzyme that degrades PHO1 (Liu *et al.*, 2012; Secco *et al.*, 2012) and perhaps also other proteins, negatively affects shoot Pi content and Pi remobilization in plants (Bartel, 2004; Aung *et al.*, 2006; Chitwood and Timmermans, 2007; Ying *et al.*, 2017). *At4* and *INDUCED BY PHOSPHATE STARVATION1* (*IPS1*) are Pi starvation-responsive long non-coding RNAs (lncRNAs), which sequester *miR399* in a 'target mimicry' manner (Franco-Zorrilla *et al.*, 2007). Under Pi-deficient conditions, increased *At4* lncRNA inhibits the cleavage of *PHO2* by *miR399*, and the up-regulated functionally intact *PHO2* transcript results in Pi translocation from shoots to roots, which benefits the development of the RSA (Fujii *et al.*, 2005; Aung *et al.*, 2006; Bari *et al.*, 2006; Bazin and Bailey-Serres, 2015). Some transcription factors have been reported to be involved in the regulation of Pi transporters. For instance, the MYB transcription factor family member MYB2 functions as a direct transcriptional activator for *miR399* in Pi starvation signaling (Baek *et al.*, 2013), and PHOSPHATE STARVATION RESPONSE1 (PHR1) initiates the up-regulation of Pi starvation-responsive genes (Rubio *et al.*, 2001). In addition, WRKY6 was identified to inhibit *PHO1* expression as a transcriptional repressor (Chen *et al.*, 2009).

Studies have shown that epigenetic mechanisms play important roles in regulating plant biotic and abiotic stress responses (Ahmad *et al.*, 2010; Sahu *et al.*, 2013; Secco *et al.*, 2017). Nuclear actin-related protein ARP6 is an essential component of the SWR1 chromatin remodeling complex, which regulates transcription via deposition of the H2A.Z histone variant into chromatin. Derepression of target loci including PSR genes in the *arp6* mutant is correlated with the presence of Pi starvation-related phenotypes, which provides a link between chromatin remodeling and the PSR (Smith *et al.*, 2010). In addition, recent studies demonstrate that ALFIN-LIKE 6 (AL6), a member of the Alfin1-like plant homeodomain-containing protein family (PHD finger), controls the transcription of a suite of genes critical for root hair elongation under low Pi conditions (Chandrika *et al.*, 2013). PHD fingers have been identified as effectors that specifically recognize H3K4me3 (trimethylated lysine 4 of histone H3) and H3K4me2 (Taverna *et al.*, 2006; Wysocka *et al.*, 2006; Zhang, 2006; Sims *et al.*, 2007).

Histone acetylation and deacetylation, catalyzed by histone acetyltransferases (HATs) and histone deacetylases (HDACs), are essential for gene expression regulation (Jenuwein and Allis, 2001). In Arabidopsis, mutation of the histone acetyltransferase GCN5 (general control non-repressed protein 5) causes pleiotropic defects that alter many aspects of plant development and responses to environmental conditions (Vlachonasios *et al.*, 2003; Benhamed *et al.*, 2006; Cohen *et al.*, 2009; Servet *et al.*, 2010; Hu *et al.*, 2015; Xing *et al.*, 2015; Wang *et al.*, 2016, 2018; Kim *et al.*, 2018; Zheng *et al.*, 2018). Studies showed that mutation of GCN5 resulted in a long-hypocotyl phenotype and reduced light-inducible gene expression, whereas mutation of histone deacetylase HDA19, an RPD3-containing HDAC, induced opposite effects (Benhamed *et al.*, 2006). Antisense inhibition or mutation of *HDA19* leads to a range of developmental abnormalities, including early senescence, serrated leaves, the formation of aerial rosettes, and delayed flowering accompanied by defects in floral organ identity (Wu *et al.*, 2000a, b; Tian and Chen, 2001). Recently, a group reported that HDA19 modulates a subset of PSRs by regulating genes encoding SPX domain-containing proteins and genes involved in lipid remodeling (Chen *et al.*, 2015). Here, we aimed to investigate the regulation of the PSR by histone acetylation in Arabidopsis. For this purpose, we explored the effects of GCN5 on Pi-deficient responses and its functions in modulating the acetylation levels of target genes important for the PSR network.

Materials and methods

Plant materials and growth conditions

Seeds of *Arabidopsis thaliana* wild-type Ws, *gcn5-1*, and *gcn5-2* mutants (Ws background) were used in this study. The *gcn5-1* and *gcn5-2* mutants were both T-DNA insertion mutants in the bromodomain-coding region (Bertrand *et al.*, 2003; Vlachonasios *et al.*, 2003), which were kindly provided by Professor Zhou Daoxiu. For seed germination, sterilized seeds were incubated at 4 °C for 3 d; seeds were then sown on Murashige and Skoog (MS) plates containing 1% sucrose and 0.6% agar. Seedlings were grown under 16 h light/8 h dark conditions at 22 °C in a growth room. For Pi deficiency treatment, 7-day-old seedlings were transferred to MS medium containing 0.0125 mM KH_2PO_4 (1% Pi content of 1× MS) for the indicated times (Baek *et al.*, 2013).

Phosphate analysis

Pi concentrations were analyzed with molybdenum–ascorbic acid as described (Fujii *et al.*, 2005) with minor modifications. Briefly, 100 mg of fresh shoots (with the old and etiolated leaves removed) and roots homogenized in liquid nitrogen were suspended in 1 ml of solution I (100 mM NaCl, 10 mM Tris, 1 mM EDTA, 0.1% β-mercaptoethanol, pH 8.0). Nine volumes of 1% glacial acetic acid were added. After incubation at 42 °C for 30 min, the solution was centrifuged at 5000 *g* for 10 min. A 60 µl aliquot of supernatant was mixed with 140 µl of solution II [0.35% $(NH_4)_6Mo_7O_{24}{\cdot}4H_2O$, 0.86 N H_2SO_4, 1.43% ascorbic acid] and incubated at 45 °C for 20 min. Absorbance at 820 nm was measured using a BioTek Synergy HT Multi-Mode Microplate Reader (BioTek, Vermont, USA). KH_2PO_4 was used for producing the standard curve.

RNA isolation, library preparation, and transcriptome sequencing

Total RNA was extracted from 13-day-old seedlings of Ws and *gcn5-2* which had been subjected to Pi-sufficient and -deficient treatments, using TRIzol reagent (Invitrogen, Carlsbad, CA, USA), and three replicates

for each sample were analyzed. Paired end sequencing libraries with an average insert size of 200 bp were prepared with a TruSeq RNA Sample Preparation Kit v2 (Illumina, San Diego, CA, USA) and sequenced on HiSeq2000 (Illumina) according to the manufacturer's standard protocols. Raw data obtained from Illumina sequencing were analyzed as previously described, with minor modifications (Li *et al.*, 2016). In brief, each library was mapped independently using TopHat version 2.0.12 (http://ccb.jhu.edu/software/tophat/index.shtml) against the *A. thaliana* genome sequence index (TAIR 10). For differential gene analyses of each comparison, Cuffdiff version 2.2.1 was run by using the reference transcriptome along with the BAM files resulting from TopHat for each sample. The genes, with changes >2-fold and a q-value <0.05, were defined as differentially expressed genes. The groups of differentially expressed genes from RNA sequencing (RNA-seq) in this study are shown in Supplementary Table S2 at *JXB* online.)

Chromatin immunoprecipitations

ChIP assays were performed as described previously (Fiil *et al.*, 2008). Arabidopsis seeds were sterilized, kept for 3 d at 4 °C, and grown *in vitro* under long-day conditions. After 7 d growth on MS medium, the seedlings were separately treated in normal or Pi deficiency conditions, and were harvested and fixed in 1% formaldehyde for 15 min in a vacuum and then neutralized by 0.125 M glycine. After washing with sterilized water, the samples were ground in liquid nitrogen. Nuclear pellets were suspended in a buffer containing 0.25 M sucrose, 10 mM Tris–HCl, pH 8, 10 mM $MgCl_2$, 1% Triton X-100, 5 mM β-mercaptoethanol, 0.1 mM phenylmethylsulfonyl fluoride (PMSF), and protease inhibitors (one mini tablet per ml; Roche). The suspensions were transferred to microfuge tubes and centrifuged at 12 000 *g* for 10 min. The pellets were suspended in 1.7 M sucrose, 10 mM Tris–HCl, pH 8, 2 mM $MgCl_2$, 0.15% Triton X-100, 5 mM β-mercaptoethanol, 0.1 mM PMSF, and protease inhibitors, and centrifuged through a layer of the same buffer in microfuge tubes. The nuclear pellets were lysed in a buffer containing 50 mM Tris–HCl, pH 8, 10 mM EDTA, 1% SDS, and protease inhibitors. The lysed nuclei were sonicated four times for 15 s at 4 °C followed by centrifugation. The supernatants containing chromatin fragments were diluted 10-fold with 1% Triton X-100, 1.2 mM EDTA, 16.7 mM Tris–HCl, pH 8, and 167 mM NaCl. Aliquots of the dilution were used for an immunoprecipitation assay.

The GCN5 antibody was kindly provided by Professor Zhou Daoxiu, and its specificity was confirmed by protein gel blots (Benhamed *et al.*, 2006, 2008). The H3K14ac (Cat no. A-4023-025) and H3K9ac (Cat no. A-4022-025) antibodies were bought from Upstate Biotechnology. *CHS* was amplified as an endogenous control. Immunoprecipitated DNA was analyzed by PCR using the primer sets listed in Supplementary Table S1, and amplified DNA from the chromatin fractions prior to antibody incubation were used as the controls (inputs). The fold enrichment was normalized to the chromatin inputs.

Examination of miR399

Total RNA was extracted with TRIzol reagent (Invitrogen) according to the manufacturer's instructions. A stem–loop reverse transcription–PCR (RT–PCR) was performed to quantify miR399 as previously described (Chen *et al.*, 2005). Quantitative real-time PCR (qRT-PCR) was conducted on a Bio-Rad IQ5 Real-Time PCR Detection System. Each reaction included 2 μl of product from the diluted reverse transcription reactions, 1.0 μl of each primer (forward and reverse), 12.5 μl of SYBR® Premix Ex Taq™ (Perfect Real Time; TaKaRa), and 8.5 μl of nuclease-free water. The reactions were incubated in a 96-well plate at 95 °C for 30 s, followed by 40 cycles of 95 °C for 5 s, 60 °C for 30 s, and 72 °C for 30 s. The specificity of the PCR-amplified *miR399f* product was proved by T-vector cloning combined with sequencing. All reactions were run in three replicates for each sample. The *ACT8* gene served as the endogenous control.

Accession numbers

Sequence data from this study can be found in the Arabidopsis Genome Initiative or GenBank/EMBL databases under the following accession numbers: *At4*, AT5G03545; *GCN5*, AT3G54610; *MYB2*, AT2G47190; *PHO2*, AT2G33770; *PHO1*, AT3G23430; *WRKY6*, AT1G62300; *MYB62*, AT1G68320; *SBT3.5*, AT1G32940; *RIPK*, AT2G05940; *PLDP2*, AT3G05630; *PLIP3*, AT3G62590; *MGD2*, AT5G20410; *ACT8*, AT1G49240; and *CHS*, AT5G13930; The RNA-seq reads used for this study are deposited at the National Center for Biotechnology Information Short Read Archive under the accession number SRP201144.

Results

gcn5 *mutants display impaired Pi deficiency responses in Arabidopsis*

In order to clarify the roles of histone acetylation for Pi deficiency responses, we screened Arabidopsis T-DNA insertion mutants for 12 genes, namely *GCN5*, *SILENT INFORMATION REGULATOR2* (*SRT2*), AT5G61050 (*MAF19.6*), *HDA2C*, *HDA5*, *HDA7*, *HDA13*, *HDA14*, *HDA15*, *HDA18*, *HDA19*, and *PKL*, which are essential modulators of the histone acetylation level in Arabidopsis. After Pi deficiency treatment (1% Pi content of 1× MS) for 6 d, we noted that both *gcn5-2* and *gcn5-1* mutant alleles (the T-DNAs were inserted in the bromodomain-coding region) showed obvious yellowish-purple leaf color compared with the wild-type Ws, which is a symptom of Pi starvation and may be connected to anthocyanin accumulation and senescence in leaves (Fig. 1A). In contrast to the significant inhibition of root growth in wild-type Ws in response to Pi deficiency, the root growth of *gcn5* mutants was slightly affected by Pi deficiency treatment (Fig. 1A, B; Supplementary Fig. S1). Moreover, the S:R of the fresh weight in *gcn5* mutants decreased significantly under low Pi conditions relative to that of the wild-type plants (Fig. 1C), indicating the more severe response to Pi deficiency in leaves of *gcn5* mutants compared with that in Ws.

Plants translocate a large proportion of Pi from the shoots to the roots to maximize Pi acquisition in response to a limiting Pi level (Ticconi and Abel, 2004). As shown in Fig. 1D, the *gcn5* mutants showed decreased Pi concentration in shoots and roots compared with Ws in both Pi-deprived and -replete conditions, but the S:R ratio of Pi was significantly up-regulated after Pi deficiency treatment (Fig. 1E), which proved that the mutation of GCN5 may impair the uptake and allocation of Pi in plants during Pi deficiency. In addition, we examined the time course expression patterns of *GCN5* during the low Pi treatment and found that *GCN5* transcripts were modestly induced by Pi deficiency and peaked after 1 d of Pi deficiency treatment (Fig. 1F). Collectively, these data suggested that GCN5 contributed to the robust PSRs in Arabidopsis.

Illumina high-throughput sequencing reveals 888 genes as GCN5-regulated candidate genes for PSRs

As a histone acetyltransferase, GCN5 generally regulates the acetylation levels of hundreds of loci in Arabidopsis (Imoberdorf *et al.*, 2006; Benhamed *et al.*, 2008). Thus, genomic-scale research was needed to interpret the complicated roles of GCN5 in PSR regulation. Because the two *gcn5* mutants showed similar phenotypes, the mutant we used for further analysis was *gcn5-2*. We applied Illumina high-throughput sequencing

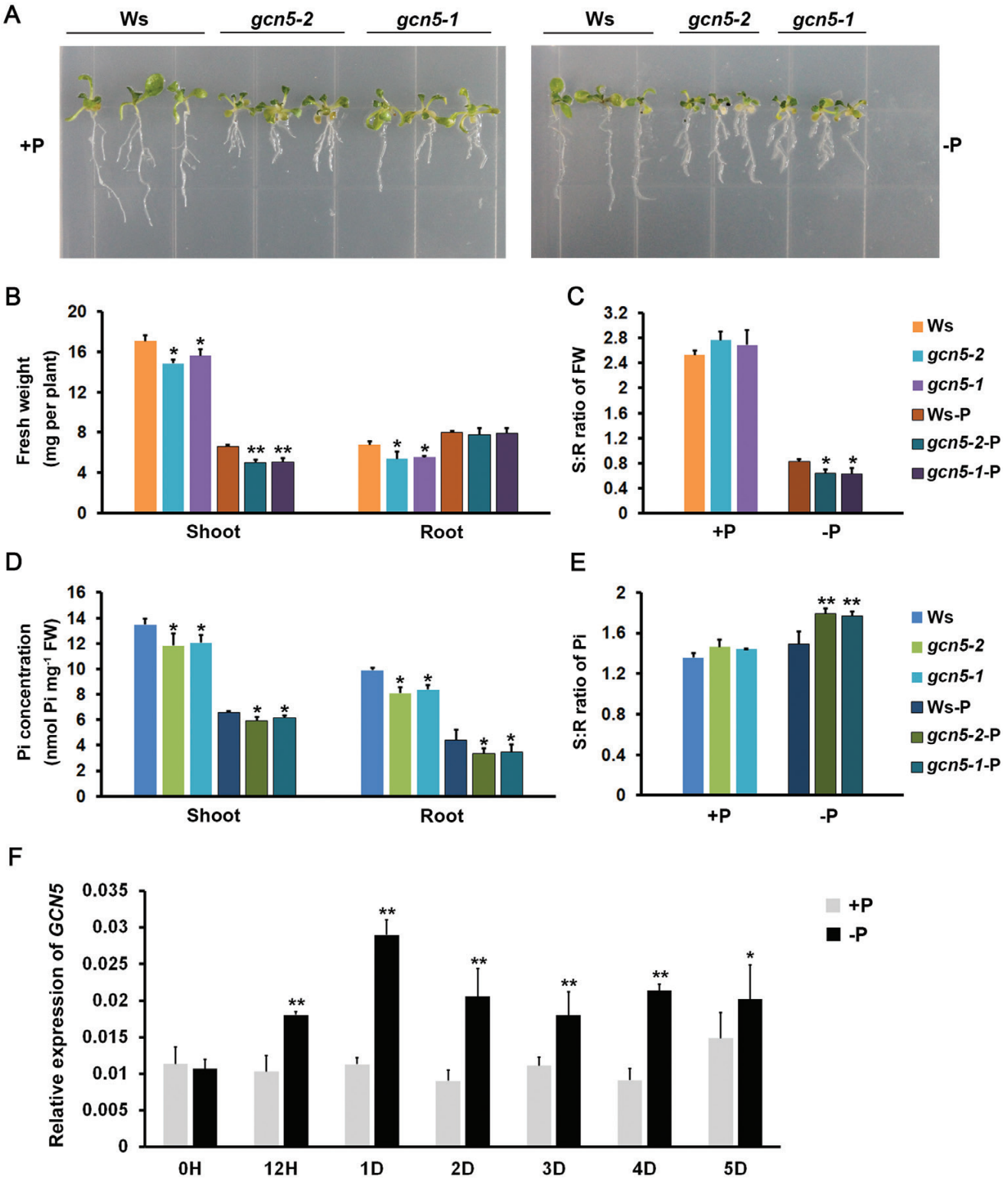

Fig. 1. GCN5 plays important roles in PSRs in Arabidopsis. (A) Seven-day-old seedlings of Ws, *gcn5-1*, and *gcn5-2* were transferred onto MS plates with sufficient Pi (+P) or deficient Pi (–P) for an additional 6 d. (B) FW and (C) shoot to root ratio (S:R) of the FW of 13-day-old seedlings of Ws, *gcn5-1*, and *gcn5-2* grown under Pi-sufficient or -deficient conditions. Values are the mean of three replicates for each sample. Bars with asterisks are significantly different from the wild-type Ws in each condition (*P<0.05, **P<0.01; Student's t-test). (D) Pi concentration and (E) S:R ratio of Pi (the ratio of the total amount of Pi in the shoot and root) are shown for shoots and roots of 13-day-old seedlings of Ws and *gcn5* grown under Pi-sufficient or -deficient conditions. Values are the mean of three replicates for each sample. Bars with asterisks are significantly different from the corresponding wild-type Ws in each condition (*P<0.05, **P<0.01; Student's t-test). (F) Seven-day-old Ws seedlings were transferred onto MS plates with deficient Pi for 0 h to 5 d. Total RNA was isolated, and qRT-PCR showed the dynamic expression of *GCN5*. The expression of *ACT8* was used to normalize mRNA levels. Error bars represent the SD values from three biological repetitions for each sample, and the experiment was repeated at least three times. Bars with asterisks are significantly different among comparisons of Pi-sufficient and -deficient treatments at different time points (**P<0.01, *P<0.05; Student's t-test). (This figure is available in color at *JXB* online.)

approaches to compare the transcription profiles of 13-day-old seedling in four conditions, designated as Ws (wild type with sufficient Pi), Ws-P (wild type with deficient Pi), *gcn5* (*gcn5* mutant with sufficient Pi), and *gcn5*-P (*gcn5* mutant with deficient Pi), respectively. With three biological replicates for each sample, the reproducibility and the accuracy of transcriptome data were validated by qRT-PCR (Supplementary Fig. S2). After Pi deficiency treatment, 3036 genes showed a dramatic response to Pi deficiency in Ws, whereas only 358 genes were changed in the *gcn5* mutant, designated as 'Ws-P/Ws' and 'gcn5-P/gcn5', respectively (Supplementary Table S2). Additionally, a total of 445 and 2461 genes were significantly changed in the *gcn5* mutant relative to Ws in Pi-replete and Pi-deprived conditions, respectively, designated as 'gcn5/Ws' and 'gcn5-P/Ws-P' (Supplementary Table S2). Comparisons of the four pairs of transcript abundances showed that genes differentially expressed in 'Ws-P/Ws' were obviously less affected in 'gcn5-P/gcn5', and exhibited the reverse expression pattern in 'gcn5-P/Ws-P' (Fig. 2A). These results suggested that the response to Pi deficiency is largely impaired in the *gcn5* mutant, indicating that GCN5 functions in the PSR.

Since GCN5 functions as a transcriptional activator (Imoberdorf *et al.*, 2006), the GCN5-regulated genes in the PSR should be incorporated in the overlap between 'Ws-P>gcn5-P' and 'Ws-P>Ws' (Fig. 2B). Among the overlapping genes, 90 genes belonged to the 'gcn5-P>gcn5' group which might not

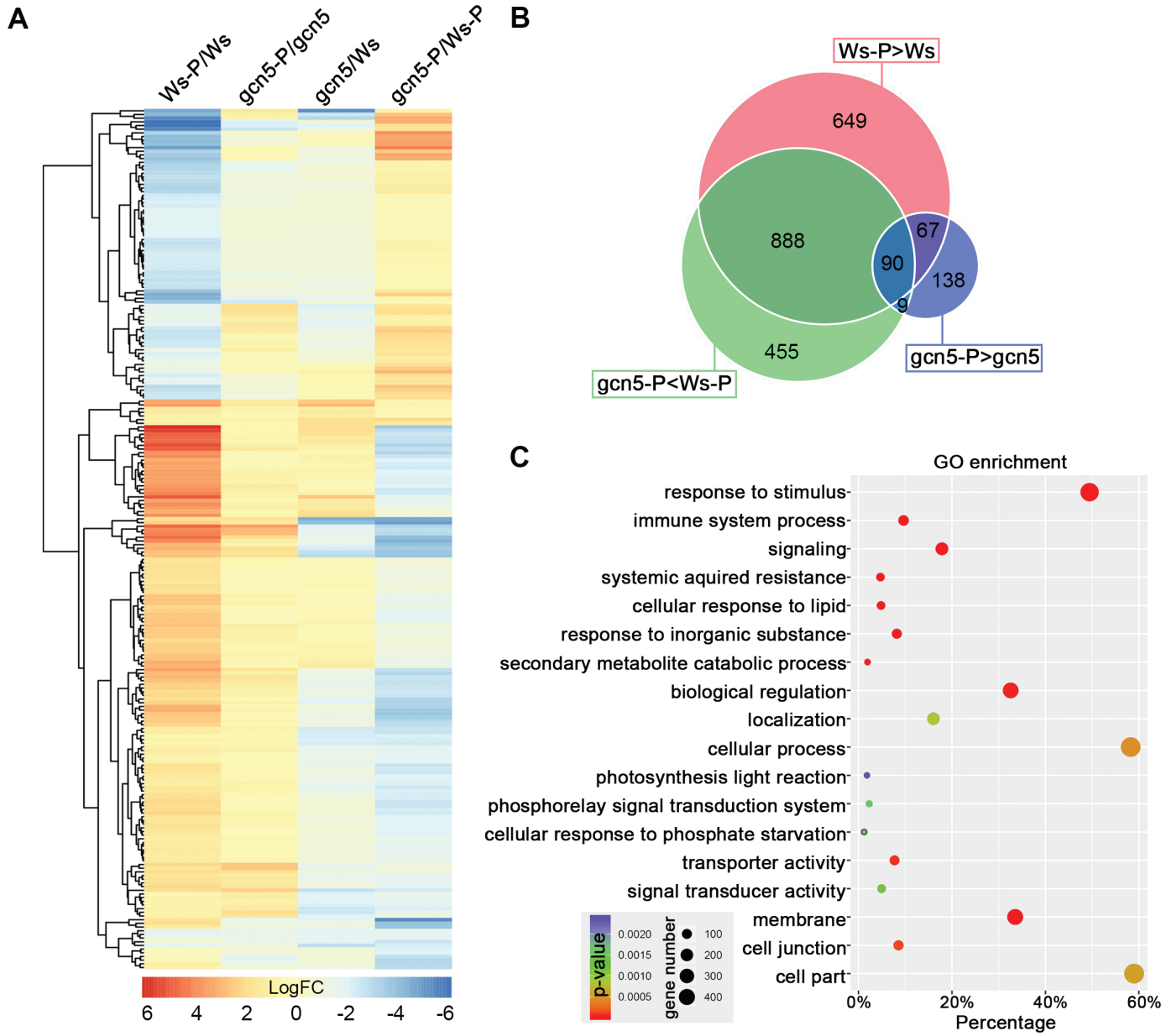

Fig. 2. Identification of the potential GCN5 targets for PSRs. (A) Heatmap of the logFC values in 'Ws-P/Ws', 'gcn5-P/gcn5', 'gcn5/Ws', and 'gcn5-P/gcn5' of genes that are differentially expressed in all four comparisons. (B) Venn diagram of the determined differentially expressed genes in each comparison, which represented potential GCN5 targets in response to Pi deficiency. (C) Summary of the over-represented GO categories (biological processes; *P*-value <0.05; Benjamini–Hochberg correction) for the 888 GCN5-regulated candidate genes, using AgriGO v2.0. The number of genes that are associated with that respective GO category and the corresponding *P*-value are represented as dots. (This figure is available in color at *JXB* online.)

be regulated by GCN5. Finally, the 888 genes were selected as GCN5-regulated candidate genes involved in the PSR (Fig. 2B). Based on Gene Ontology (GO) categories, we used AgriGO v2.0 to analyze the enrichments of function-related gene groups (Tian *et al.*, 2017). The majority (≥50%) of GCN5-regulated candidate genes had a significant enrichment [false discovery rate (FDR) <0.05] of response to stimulus, cellular process, and cell part, which includes, for example, response to inorganic substances, the phosphorelay signal transduction system, and cellular response to phosphate starvation, that may be associated with PSR mechanisms. In addition to these, a large fraction of genes implicated in membrane processes, signaling, localization, immune system, cell junction, and transporter activity were also over-represented, suggesting that the cellular signal transduction-related processes were significantly influenced (Fig. 2C; Supplementary Table S3).

Four genes are identified as direct targets of GCN5 in PSR regulation

To further clarify the relationship between GCN5 and Pi deficiency response, direct targets of GCN5 after Pi deficiency treatment need to be identified. Based on the GO analysis results, we focused on 10 candidate genes from the GO category of cellular response to phosphate starvation (Table 1), including *WRKY6*, *MYB62*, and *At4*, which were reported to play important roles in phosphate redistribution under Pi-limited or starvation conditions (Shin *et al.*, 2006; Franco-Zorrilla *et al.*, 2007; Chen *et al.*, 2009; Devaiah *et al.*, 2009). We performed ChIP assays to examine the 10 candidate genes in 13-day-old seedlings of Ws and the *gcn5* mutant under Pi deficiency by using GCN5-specific antibodies (Benhamed *et al.*, 2006, 2008). Because GCN5 is mainly responsible for the acetylation of its targets at promoters (Bertrand *et al.*, 2003; Bhat *et al.*, 2003; Earley *et al.*, 2007), primers spanning core promoter regions were used for ChIP-qPCR analysis. As shown in Fig. 3A, GCN5 significantly bound to four of the candidate genes in the wild type relative to the *gcn5* mutant, namely *WRKY6*, *SBT3.5*, *RIPK*, and *At4*.

Table 1. *The potential GCN5-regulated, Pi deficiency-induced genes*

Gene ID	Gene name	Annotation
AT1G67600		Acid phosphatase/vanadium-dependent haloperoxidase-related protein
AT1G62300	*WRKY6**	WRKY family transcription factor
AT1G19200		Cyclin-dependent kinase, putative (DUF581)
AT1G68320	*MYB62**	Myb domain protein62
AT1G32940	*SBT3.5*	Subtilase family protein
AT2G05940	*RIPK*	Protein kinase superfamily protein
AT3G05630	*PLDP2*	Phospholipase DP2
AT3G62590	*PLIP3*	PLASTID LIPAS3
AT5G03545	*At4**	Response to phosphate starvation, enhanced by the presence of IAA
AT5G20410	*MGD2*	Monogalactosyldiacylglycerol synthase2

Asterisks indicate the three well-studied genes, *WRKY6*, *MYB62*, and *At4*, which are involved in Pi homeostasis.

GCN5 is specifically responsible for H3K14ac as well as affecting the acetylation of H3K9 and H3K27 which is required for the expression of hundreds of genes (Vlachonasios *et al.*, 2003; Earley *et al.*, 2007; Benhamed *et al.*, 2008; Chen *et al.*, 2017). To further confirm the direct regulation of these four potential target genes by GCN5, we performed ChIP-qPCR assays using antibodies against H3K9ac and H3K14ac, respectively. Consistent with the known properties of GCN5 as a histone acetyltransferase, the H3K9ac and/or H3K14ac levels of the four genes decreased due to the impairment of GCN5 (Fig. 3B). As expected, the mRNA levels of these four genes also significantly decreased in *gcn5* mutants compared with the wild type under Pi-deficient conditions (Fig. 3C). Taken together, we concluded that GCN5 directly associated with these four loci, modulated their H3K9ac and/or H3K14ac levels, and in turn regulated their expression.

The regulation of acetylation of GCN5 affects the induction of At4 *under Pi-deficient conditions*

Given the fact that H3K9/14ac levels and the expression of *At4* were significantly impaired in the *gcn5* mutant (our data) and that *At4* participates in the control of phosphate in Arabidopsis (Burleigh and Harrison, 1999; Shin *et al.*, 2006), we considered that *At4* could be an important target for GCN5 in PSRs. Consistent with the up-regulation of *GCN5*, *At4* was significantly induced 1 d later than *GCN5* and reached its highest expression level 2–3 d after phosphate withdrawal (Figs 4A, 1F), implying that *At4* might be the target gene for GCN5. To investigate how the induction of *GCN5* affected *At4* transcription, we performed ChIP experiments using an antibody against H3K14 acetylation. In support of our hypothesis, we found that H3K14ac accumulated to a higher level at the core region of the *At4* promoter under Pi-deficient conditions, and reached ~2-fold the level than that under Pi-sufficient conditions at 1–2 d time points (Fig. 4B). Collectively, these results assigned a key role for GCN5 in *At4* induction under Pi deficiency conditions. By performing another ChIP assay using the GCN5 antibody, we showed that the enrichment of GCN5 protein on the *At4* promoter was elevated in a time-dependent manner after Pi withdrawal and reached the highest level 2 d after treatment (Fig. 4C). To investigate further whether GCN5 binds to *At4* before Pi treatment, we performed a ChIP assay to examine the H3K14ac levels of the *At4* promoter and gene body regions in the wild type and *gcn5* mutants. In Pi-sufficient plants, the H3K14 acetylation of *At4* was decreased dramatically at the promoter region and modestly at the gene body region in the *gcn5* mutant under normal conditions (Fig. 4D). Altogether, these results demonstrated that GCN5 directly interacted with the *At4* promoter and promoted the robust induction of *At4* expression in response to Pi deficiency by modulating its H3K14ac level.

The contribution of At4 *to the GCN5-regulated PSR network*

To confirm whether *At4* is the direct target of GCN5 during the phosphate-deficient response, *At4* was constitutively

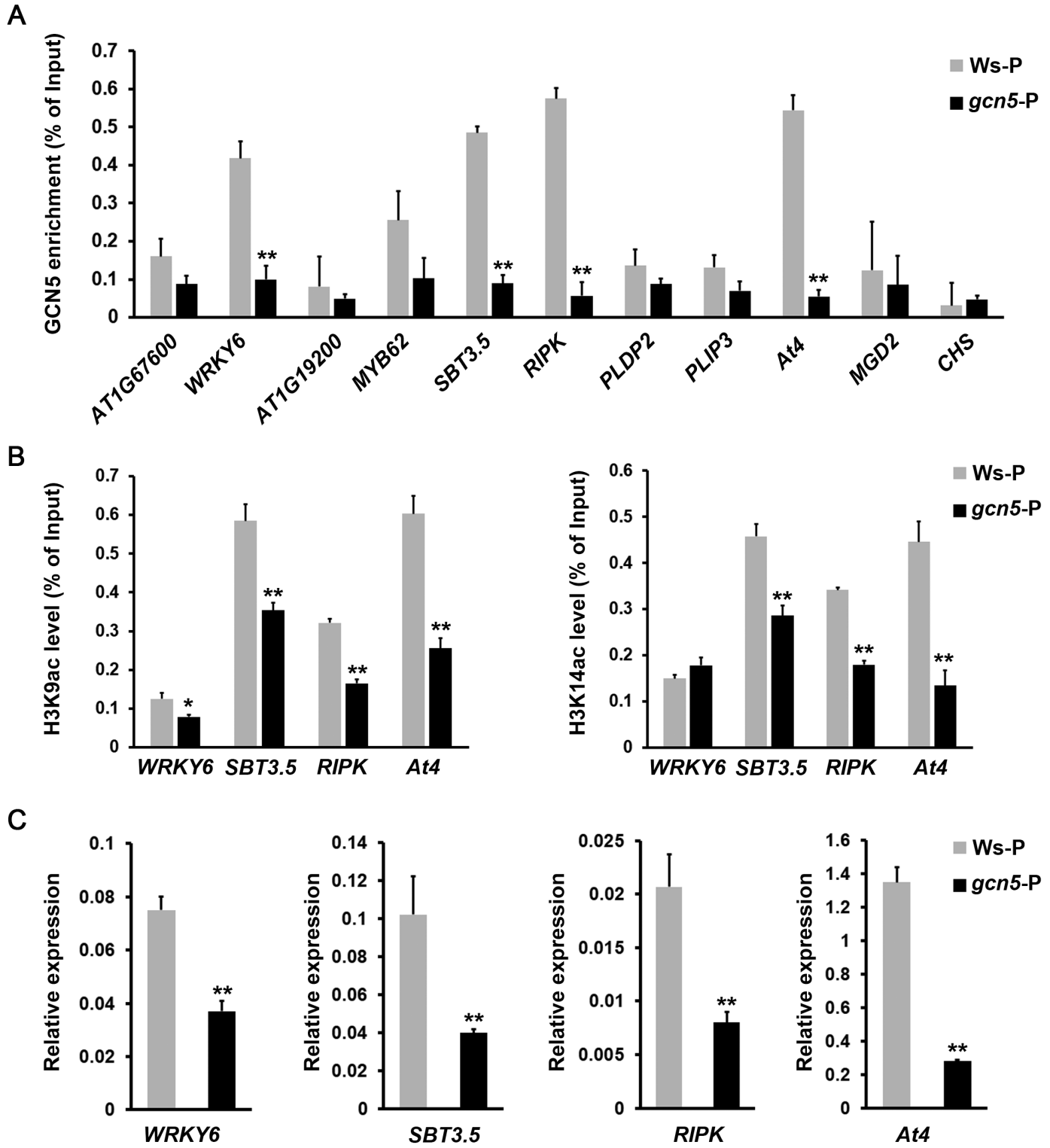

Fig. 3. Identification of the direct targets of GCN5 and measurement of their acetylation states. Seven-day-old seedlings of Ws and *gcn5* mutants were separately transferred onto MS plates with deficient Pi for 3 d. Nuclei were extracted from the cross-linked seedlings, sonicated, and immunoprecipitated with antibodies specific to GCN5, H3K9ac, and H3K14ac, respectively. Primers were designed at the core promoter region. (A) ChIP assay (anti-GCN5) to identify the direct target of GCN5. Asterisks indicated significant differences in enrichment in the *gcn5* mutant compared with that in wild-type Ws. *CHS*, whose expression is not affected by GCN5, was used as a negative control. (B) ChIP assay (anti-H3K9ac or anti-H3K14ac) to examine the H3K9ac or H3K14ac states of the four GCN5 target genes. Asterisks indicated significant differences in histone acetylation level in the *gcn5* mutant compared with that in wild-type Ws. (C) qRT-PCR to show the expression of GCN5 target genes. Error bars represent SD values from three biological repetitions for each sample, and the experiment was repeated at least three times (**P<0.01; Student's t-test).

overexpressed in *gcn5* mutants. Since it was difficult to directly obtain *35S:At4/gcn5* transgenic plants due to the low viability of *gcn5* pollen, we firstly generated *35S:At4*/Ws transgenic lines. Two independent *35S:At4*/Ws (#19 and #23) transgenic lines which exhibited the highest *At4* transcript abundance were selected for further analysis (Supplementary Fig.

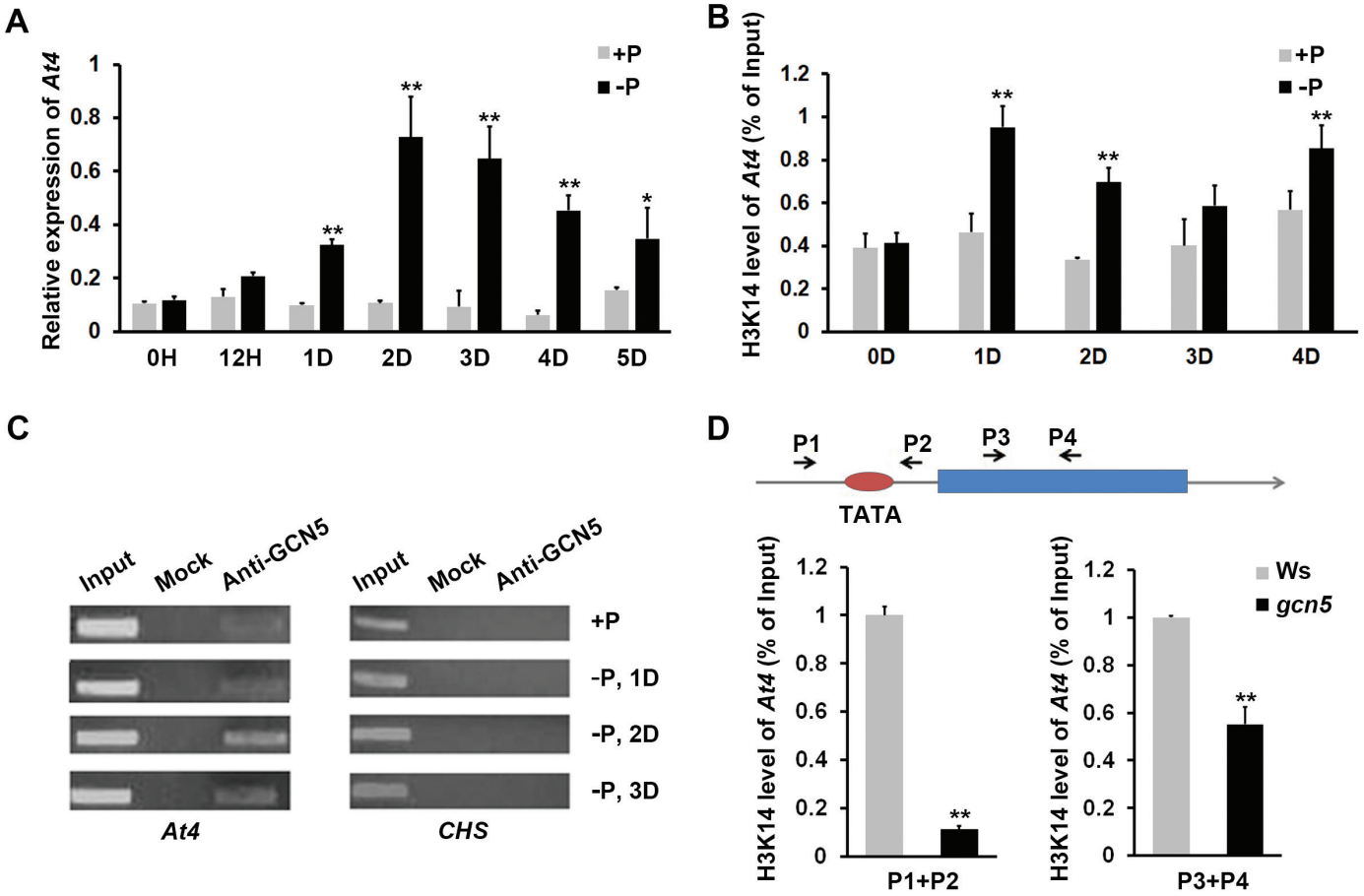

Fig. 4. GCN5 directly regulates *At4* dynamic expression through histone acetylation under Pi deficiency conditions. (A) Seven-day-old Ws seedlings were transferred onto MS plates with sufficient Pi (+P) or deficient Pi (–P) for 0 h to 5 d. Total RNA was isolated, and qRT-PCR showed the dynamic expression of *At4* transcripts. The expression of *ACT8* was used to normalize mRNA levels. Error bars represent SD values from three biological repetitions for each sample, and the experiment was repeated at least three times (**P*<0.05, ***P*<0.01; Student's *t*-test). (B) We examined the H3K14 acetylation state on the *At4* promoter of Ws in normal conditions and after 0, 1, 2, 3, and 4 d of Pi deficiency treatments. Error bars represent SD values from three biological repetitions for each sample, and the experiment was repeated at least three times (***P*<0.01; Student's *t*-test). (C) ChIP was performed to examine the enrichment of GCN5 on the *At4* promoter; *CHS* was used as a negative control. (D) ChIP was performed to examine the H3K14ac state on the *At4* promoter and gene body region before Pi-deprived treatment; P1–P2 and P3–P4 indicated the primers designed for promoter and gene body examinations, respectively. Error bars represent SD values from three biological repetitions for each sample, and the experiment was repeated at least three times (***P*<0.01; Student's *t*-test). (This figure is available in color at *JXB* online.)

S3A). Notably, *PHO2* mRNA levels were significantly elevated along with the overexpression of *At4* in these two lines (Supplementary Fig. S3B). By crossing the *gcn5* mutant with *35S:At4*/Ws transgenic lines, we successfully overexpressed *At4* in the *gcn5* mutant.

At4 and *IPS1* have been reported to function in Pi homeostasis by sequestering *miR399* via 'target mimicry' (Shin *et al.*, 2006; Franco-Zorrilla *et al.*, 2007). There are six loci in total identified as *miR399* family genes in Arabidopsis, and all of them could target *PHO2*, which has five sequences complementary to *miR399* in its 5'UTR (Lee *et al.*, 1993; Aharoni *et al.*, 2004). Among them, *miR399f* was the first member which was reported to be involved in the PSR (Koornneef *et al.*, 1989). In low Pi conditions, the *miR399f* could be detected at a much higher level in the *gcn5* mutant compared with Ws (Fig. 5A), and the abundance of *miR399d* and *miR399e* was also increased (Supplementary Fig. S3C). Moreover, *miR399f* abundance was decreased along with the overexpression of *At4* in the *gcn5* mutant background (Fig. 5A). It should be noted that the primary transcripts of *miR399f* were significantly down-regulated in the *gcn5* mutant compared with the wild type and *35S:At4/gcn5* transgenic lines in Pi-deprived conditions (Fig. 5B). It has been reported that *MYB2* encodes a transcription factor of *miR399f* and positively regulates its expression (Raffaele *et al.*, 2008); qRT-PCR results showed that the expression level of *MYB2* was significantly decreased in *gcn5* mutants in both Pi-replete and Pi-deprived conditions (Fig. 5C). These results revealed that the expression pattern of *miR399f* was different from that of *pri-miR399f* and *MYB2* in *gcn5* mutants. Previous studies showed that mature *miR399* binds to the 5'UTR of *PHO2* transcripts, leading to the degradation of *PHO2* mRNA (Fujii *et al.*, 2005; Aung *et al.*, 2006). The intact *PHO2* mRNA decreased in *gcn5* mutants but could be rescued up to nearly the wild-type level in *35S:At4/gcn5* transgenic lines under Pi deficiency treatment (Fig. 5D). All these data indicated that the decreased expression of *At4* in *gcn5* mutants caused the changes in *miR399* abundance and *PHO2* expression pattern.

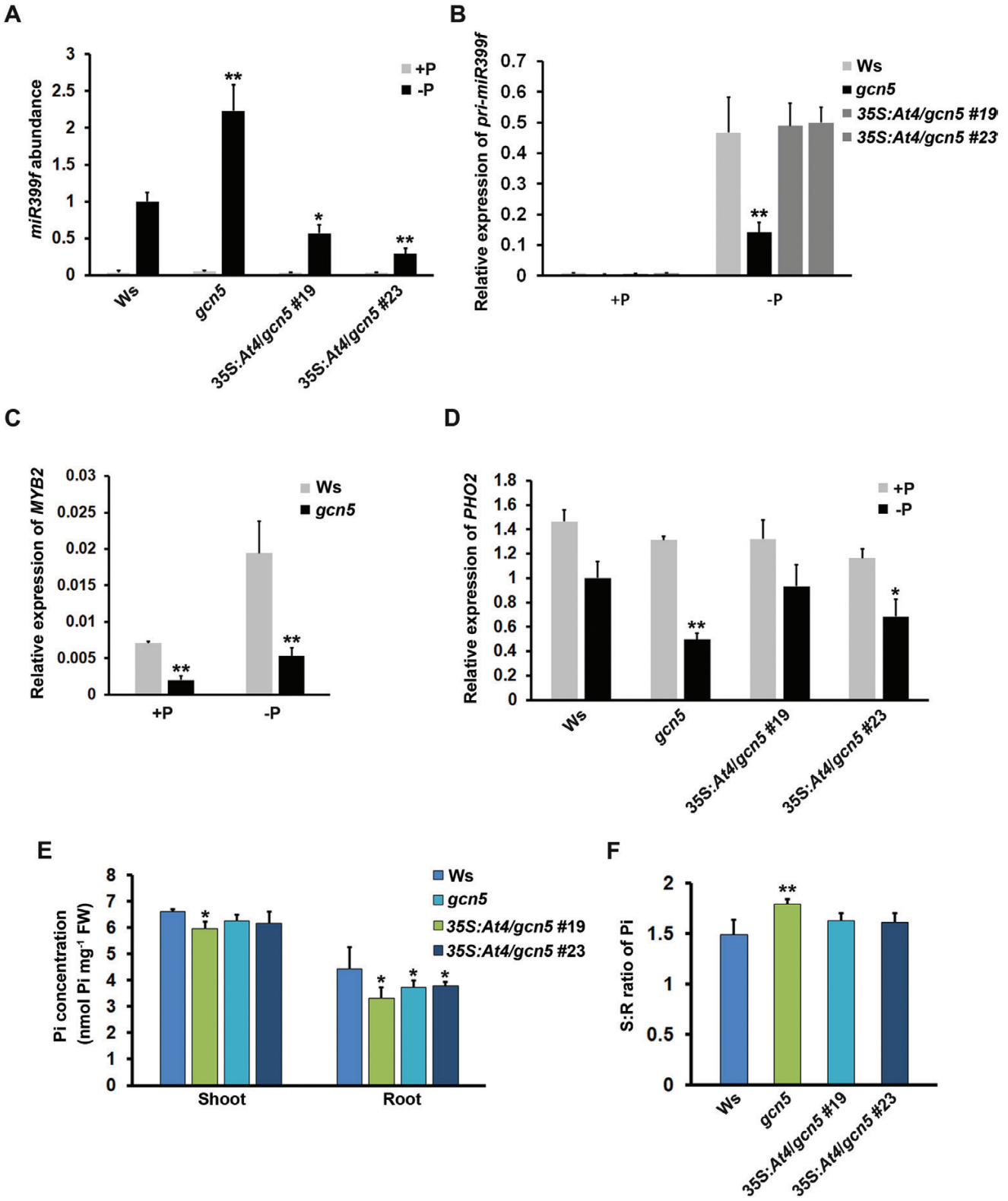

Fig. 5. Examination of *miR399* and *PHO2* transcript abundance and Pi concentration in shoots and roots. Total RNA were isolated from 13-day-old seedlings of Ws, *gcn5*, and *35S:At4/gcn5* transgenic lines grown under Pi-sufficient or -deficient conditions. (A) The *miR399f* abundance was detected by stem–loop qRT–PCR. (B) Transcript abundance of *pri-miR399f* expression in Ws, *gcn5*, and *35S:At4/gcn5* transgenic lines was detected by qRT-PCR. (C) The expression level of *MYB2* was detected by qRT-PCR in Ws and *gcn5* under normal conditions. (D) Examination of *PHO2* mRNA in Ws, *gcn5*, and *35S:At4/gcn5* transgenic lines grown under Pi-sufficient or -deficient conditions was performed by qRT-PCR. The expression of *ACT8* was used to normalize mRNA levels. Error bars represent SD values from three biological repetitions for each sample, and the experiment was repeated at least three times (**P*<0.05, ***P*<0.01; Student's *t*-test). (E) Pi concentration and (F) S:R ratio of Pi (the ratio of the total amount of Pi in the shoot and root) are shown for shoots and roots of 13-day-old seedlings in Ws, *gcn5*, and *35S:At4/gcn5* plants grown under Pi-deficient conditions. Values are the mean of three replicates for each sample. Bars with asterisks are significantly different from the corresponding wild-type Ws in each comparison (**P*<0.05, ***P*<0.01; Student's *t*-test). (This figure is available in color at *JXB* online.)

The phosphate signaling pathway defined by *At4–miR399–PHO2* contributed to Pi translocation from shoots to roots under Pi-deficient conditions, which benefits the development of RSAs (Fujii *et al.*, 2005; Aung *et al.*, 2006; Bari *et al.*, 2006; Bazin and Bailey-Serres, 2015). To investigate the phosphate translocation ability of Ws, *gcn5*, and *35S:At4/gcn5* under Pi-deficient condition, we measured the Pi concentration of shoots and roots, and further compared the S:R ratio of Pi. Overexpression of *At4* in *gcn5* could partially rescue the phosphate translocation defect between shoots and roots (Fig. 5E, F). Taken together, these data provided genetic evidence that GCN5 regulated phosphate accumulation, at least partially, by controlling the expression of *At4* in Arabidopsis.

Discussion

Histone acetyltransferase GCN5 is required for PSRs in Arabidopsis

Phosphate availability is a major factor limiting the growth, development, and productivity of plants (Rouached *et al.*, 2010; Yang and Finnegan, 2010; Chiou and Lin, 2011; Gu *et al.*, 2016; Secco *et al.*, 2017). Recently, histone 'writers' and 'readers' are reported to be involved in the PSR network (Smith *et al.*, 2010; Chandrika *et al.*, 2013; Chen *et al.*, 2015). Here, we reported that the histone acetyltransferase GCN5 is required for PSRs in Arabidopsis based on the following observations: (i) compared with the wild type, *gcn5* mutants exhibited severe symptoms of Pi deficiency after low Pi treatment; (ii) the *GCN5* transcript was up-regulated after Pi deficiency treatment; (iii) expression of 888 genes was significantly down-regulated due to the disruption of GCN5 under Pi deficiency condition; and (iv) four genes involved in phosphate homeostasis, including the well-studied *At4* and *WRKY6*, were identified as direct targets of GCN5, and H3K9ac and/or H3K14ac levels of these four genes were decreased in *gcn5* mutants.

To control gene expression accurately, histone acetyltransferases and deacetylases often cooperate with each other in gene regulation (Jenuwein and Allis, 2001). Previous studies showed that HDA19 and GCN5 function in some common targets but lead to the opposite effects (Benhamed *et al.*, 2006; Tanaka *et al.*, 2008). Chen *et al.* (2015) reported that histone deacetylase HDA19 affects leaf responses to Pi starvation, and mutants and RNAi lines of HDA19 exhibited reduced anthocyanin levels compared with the wild-type control in low Pi conditions (Chen *et al.*, 2015). The regulation of HDA19 in Pi-deprived condition is opposite to that of GCN5 which we observed in this study, which may further confirm that histone acetylation mediated by GCN5 and HDA19 functions in Pi regulation.

GCN5-mediated epigenetic regulation of lncRNA At4 *plays an important role in phosphate accumulation*

LncRNA refers to a functional RNA molecule >200 nt that will not be translated into proteins. Growing numbers of lncRNAs are being reported to have regulatory roles in various developmental processes (Mercer *et al.*, 2009; Bazin and Bailey-Serres, 2015). To date, at least four divergent lncRNA-mediated regulation mechanisms have been unraveled, namely target mimicry, interference with transcription, the POLYCOMB REPRESSIVE COMPLEX2-associated histone methylation, and DNA methylation (Zhang *et al.*, 2013). In Arabidopsis, the non-protein-coding genes *IPS1* and *At4* are induced by phosphate starvation, and they could block the repressive role of *miR399* on its target gene *PHO2*, which then regulates the dynamic balance of phosphate in shoots (Franco-Zorrilla *et al.*, 2007). However, the underlying mechanism for the up-regulation of the lncRNA *At4* after phosphate deficiency remains elusive. In this study, we found that Pi deficiency-induced GCN5 was responsible for the robust response of *At4* by enhancing its association with the *At4* promoter and concomitantly its H3K14 acetylation level. Moreover, the direct binding of GCN5 to *At4* was reported previously (Benhamed *et al.*, 2008).

Along with the decreased *At4* expression in *gcn5* mutants, *miR399* accumulation was >2-fold higher than that in the wild type, and this effect was decreased after overexpression of *At4* in the *gcn5* background in Pi deficiency condition. Further experiments with *pri-miR399* and *MYB2* showed opposite expression behavior compared with mature *miR399*, which suggested the significance of *At4* in the post-transcriptional regulation of *miR399f*. As expected, *PHO2*, the target of *miR399*, was down-regulated in *gcn5* mutants, and the S:R ratio of Pi in *gcn5* mutants was significantly increased compared with the wild type. In addition, overexpression of *At4* in *gcn5* could partially rescue these Pi impairments. Although the phosphate translocation could be elucidated by GCN5-regulated *At4* expression, the Pi concentrations of shoots and roots in *gcn5* mutants were both decreased under Pi-sufficient conditions, indicating our limited understanding of the complex role of GCN5 in Pi accumulation, which requires further investigation.

We propose that GCN5 is involved in PSR by modulating *At4* expression. Remarkably, the link between GCN5 and *At4* provides a new epigenetic mechanism for the regulation of lncRNA in plants. However, GCN5 controls histone acetylation of hundreds of loci (Benhamed *et al.*, 2008), and in this study we identified four targets of GCN5 involved in the

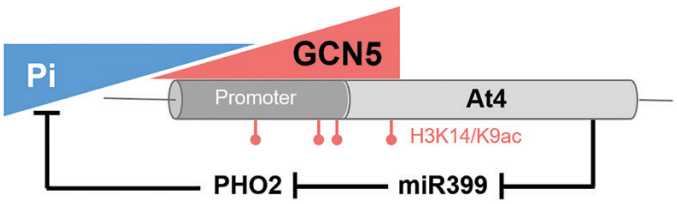

Fig. 6. A simple model for GCN5 regulation of PSR in Arabidopsis. Pi deficiency could induce the expression of *GCN5*, which facilitates the expression of the GCN5 direct target *At4* by up-regulating its H3K14/K9 acetylation levels. Concomitantly, followed by the inhibition of *miR399*, the *PHO2* mRNA level was increased, resulting in the impairment of Pi accumulation in plants. The two triangles represent the external Pi supply and the histone acetyltransferase GCN5. The schematic of lncRNA *At4* (light gray) and its promoter region (dark gray) shows histone H3K14/K9ac modifications. Solid black arrows represent the GCN5-involved regulation of the PSR pathway. (This figure is available in color at *JXB* online.)

phosphate deficiency response. Thus, to gain a comprehensive interpretation of the role of GCN5 in Pi homeostasis, it is necessary to study other GCN5 target genes in this process. In summary, we proposed a model of GCN5-mediated regulation of lncRNA *At4* contributing to PSR in Arabidopsis (Fig. 6). Briefly, Pi deficiency-induced GCN5 positively regulates the expression of lncRNA *At4* by modulating its histone acetylation. This epigenetic regulation of *At4* could affect mature *miR399* abundance, thus the functionally intact *PHO2* mRNA level, and finally the efficiency of Pi allocation and Pi accumulation in plant.

Supplementary data

Supplementary data are available at *JXB* online.

Table S1. Gene-specific primer pairs used in this study.

Table S2. The groups of differentially expressed genes from RNA-seq.

Table S3. The significantly enriched Gene Ontology groups.

Fig. S1. Observation of primary root length and lateral root number of Ws and *gcn5* in Pi-replete and Pi-deprived conditions.

Fig. S2. Eight genes selected to examine the accuracy of RNA-seq using qRT-PCR.

Fig. S3. Examination of *At4* and *PHO2* expression and mature *miR399* abundance.

Acknowledgements

We thank Qixin Sun for providing constructive comments on the manuscript, and Shunong Bai for providing seeds. This work was supported by the Ministry of Agriculture of China for Transgenic Research (2016ZX08009002) and the State Key Laboratory of Agrobiotechnology Open Grant (2018SKLAB6-25). All authors have no conflicts of interest to declare.

References

Aharoni A, Dixit S, Jetter R, Thoenes E, van Arkel G, Pereira A. 2004. The SHINE clade of AP2 domain transcription factors activates wax biosynthesis, alters cuticle properties, and confers drought tolerance when overexpressed in Arabidopsis. The Plant Cell **16**, 2463–2480.

Ahmad A, Zhang Y, Cao XF. 2010. Decoding the epigenetic language of plant development. Molecular Plant **3**, 719–728.

Aung K, Lin SI, Wu CC, Huang YT, Su CL, Chiou TJ. 2006. pho2, a phosphate overaccumulator, is caused by a nonsense mutation in a microRNA399 target gene. Plant Physiology **141**, 1000–1011.

Baek D, Kim MC, Chun HJ, *et al*. 2013. Regulation of miR399f transcription by AtMYB2 affects phosphate starvation responses in Arabidopsis. Plant Physiology **161**, 362–373.

Bari R, Datt Pant B, Stitt M, Scheible WR. 2006. PHO2, microRNA399, and PHR1 define a phosphate-signaling pathway in plants. Plant Physiology **141**, 988–999.

Bartel DP. 2004. MicroRNAs: genomics, biogenesis, mechanism, and function. Cell **116**, 281–297.

Bazin J, Bailey-Serres J. 2015. Emerging roles of long non-coding RNA in root developmental plasticity and regulation of phosphate homeostasis. Frontiers in Plant Science **6**, 400.

Benhamed M, Bertrand C, Servet C, Zhou DX. 2006. Arabidopsis GCN5, HD1, and TAF1/HAF2 interact to regulate histone acetylation required for light-responsive gene expression. The Plant Cell **18**, 2893–2903.

Benhamed M, Martin-Magniette ML, Taconnat L, *et al*. 2008. Genome-scale Arabidopsis promoter array identifies targets of the histone acetyltransferase GCN5. The Plant Journal **56**, 493–504.

Bertrand C, Bergounioux C, Domenichini S, Delarue M, Zhou DX. 2003. Arabidopsis histone acetyltransferase AtGCN5 regulates the floral meristem activity through the WUSCHEL/AGAMOUS pathway. Journal of Biological Chemistry **278**, 28246–28251.

Bhat RA, Riehl M, Santandrea G, Velasco R, Slocombe S, Donn G, Steinbiss HH, Thompson RD, Becker HA. 2003. Alteration of GCN5 levels in maize reveals dynamic responses to manipulating histone acetylation. The Plant Journal **33**, 455–469.

Burleigh SH, Harrison MJ. 1999. The down-regulation of Mt4-like genes by phosphate fertilization occurs systemically and involves phosphate translocation to the shoots. Plant Physiology **119**, 241–248.

Chandrika NN, Sundaravelpandian K, Yu SM, Schmidt W. 2013. ALFIN-LIKE 6 is involved in root hair elongation during phosphate deficiency in Arabidopsis. New Phytologist **198**, 709–720.

Chen C, Li C, Wang Y, *et al*. 2017. Cytosolic acetyl-CoA promotes histone acetylation predominantly at H3K27 in Arabidopsis. Nature Plants **3**, 814–824.

Chen C, Ridzon DA, Broomer AJ, *et al*. 2005. Real-time quantification of microRNAs by stem–loop RT–PCR. Nucleic Acids Research **33**, e179.

Chen CY, Wu K, Schmidt W. 2015. The histone deacetylase HDA19 controls root cell elongation and modulates a subset of phosphate starvation responses in Arabidopsis. Scientific Reports **5**, 15708.

Chen YF, Li LQ, Xu Q, Kong YH, Wang H, Wu WH. 2009. The WRKY6 transcription factor modulates PHOSPHATE1 expression in response to low Pi stress in Arabidopsis. The Plant Cell **21**, 3554–3566.

Chiou TJ, Lin SI. 2011. Signaling network in sensing phosphate availability in plants. Annual Review of Plant Biology **62**, 185–206.

Chitwood DH, Timmermans MC. 2007. Target mimics modulate miRNAs. Nature Genetics **39**, 935–936.

Cohen R, Schocken J, Kaldis A, Vlachonasios KE, Hark AT, McCain ER. 2009. The histone acetyltransferase GCN5 affects the inflorescence meristem and stamen development in Arabidopsis. Planta **230**, 1207–1221.

Devaiah BN, Madhuvanthi R, Karthikeyan AS, Raghothama KG. 2009. Phosphate starvation responses and gibberellic acid biosynthesis are regulated by the MYB62 transcription factor in Arabidopsis. Molecular Plant **2**, 43–58.

Du Q, Wang K, Zou C, Xu C, Li WX. 2018. The PILNCR1–miR399 regulatory module is important for low phosphate tolerance in maize. Plant Physiology **177**, 1743–1753.

Earley KW, Shook MS, Brower-Toland B, Hicks L, Pikaard CS. 2007. In vitro specificities of Arabidopsis co-activator histone acetyltransferases: implications for histone hyperacetylation in gene activation. The Plant Journal **52**, 615–626.

Fang Z, Shao C, Meng Y, Wu P, Chen M. 2009. Phosphate signaling in Arabidopsis and *Oryza sativa*. Plant Science **176**, 170–180.

Fiil BK, Qiu JL, Petersen K, Petersen M, Mundy J. 2008. Coimmunoprecipitation (co-IP) of nuclear proteins and chromatin immunoprecipitation (ChIP) from Arabidopsis. Cold Spring Harbor Protocols **2008**, pdb.prot5049.

Franco-Zorrilla JM, Valli A, Todesco M, *et al*. 2007. Target mimicry provides a new mechanism for regulation of microRNA activity. Nature Genetics **39**, 1033–1037.

Fujii H, Chiou TJ, Lin SI, Aung K, Zhu JK. 2005. A miRNA involved in phosphate-starvation response in Arabidopsis. Current Biology **15**, 2038–2043.

Gu M, Chen A, Sun S, Xu G. 2016. Complex regulation of plant phosphate transporters and the gap between molecular mechanisms and practical application: what is missing? Molecular Plant **9**, 396–416.

Hu Z, Song N, Zheng M, *et al*. 2015. Histone acetyltransferase GCN5 is essential for heat stress-responsive gene activation and thermotolerance in Arabidopsis. The Plant Journal **84**, 1178–1191.

Imoberdorf RM, Topalidou I, Strubin M. 2006. A role for gcn5-mediated global histone acetylation in transcriptional regulation. Molecular and Cellular Biology **26**, 1610–1616.

Jenuwein T, Allis CD. 2001. Translating the histone code. Science **293**, 1074–1080.

Kim JY, Yang W, Forner J, Lohmann JU, Noh B, Noh YS. 2018. Epigenetic reprogramming by histone acetyltransferase HAG1/AtGCN5 is required for pluripotency acquisition in Arabidopsis. The EMBO Journal **37**, e98726.

Koornneef M, Hanhart CJ, Thiel F. 1989. A genetic and phenotypic description of eceriferum mutants in *Arabidopsis thaliana*. Journal of Heredity **80**, 118–122.

Lambers H, Cramer MD, Shane MW, Wouterlood M, Poot P, Veneklaas EJ. 2003. Introduction: structure and functioning of cluster roots and plant responses to phosphate deficiency. Plant and Soil **248**, ix–xix.

Lambers H, Shane MW, Cramer MD, Pearse SJ, Veneklaas EJ. 2006. Root structure and functioning for efficient acquisition of phosphorus: matching morphological and physiological traits. Annals of Botany **98**, 693–713.

Lee DY, Hayes JJ, Pruss D, Wolffe AP. 1993. A positive role for histone acetylation in transcription factor access to nucleosomal DNA. Cell **72**, 73–84.

Li S, Wang X, He S, *et al*. 2016. CFLAP1 and CFLAP2 are two bHLH transcription factors participating in synergistic regulation of AtCFL1-mediated cuticle development in Arabidopsis. PLoS Genetics **12**, 1–27.

Liang C, Wang J, Zhao J, Tian J, Liao H. 2014. Control of phosphate homeostasis through gene regulation in crops. Current Opinion in Plant Biology **21**, 59–66.

Lin SI, Chiang SF, Lin WY, Chen JW, Tseng CY, Wu PC, Chiou TJ. 2008. Regulatory network of microRNA399 and PHO2 by systemic signaling. Plant Physiology **147**, 732–746.

Lin WY, Lin SI, Chiou TJ. 2009. Molecular regulators of phosphate homeostasis in plants. Journal of Experimental Botany **60**, 1427–1438.

Liu TY, Huang TK, Tseng CY, Lai YS, Lin SI, Lin WY, Chen JW, Chiou TJ. 2012. PHO2-dependent degradation of PHO1 modulates phosphate homeostasis in Arabidopsis. The Plant Cell **24**, 2168–2183.

Mercer TR, Dinger ME, Mattick JS. 2009. Long non-coding RNAs: insights into functions. Nature Reviews. Genetics **10**, 155–159.

Raffaele S, Vailleau F, Léger A, Joubès J, Miersch O, Huard C, Blée E, Mongrand S, Domergue F, Roby D. 2008. A MYB transcription factor regulates very-long-chain fatty acid biosynthesis for activation of the hypersensitive cell death response in Arabidopsis. The Plant Cell **20**, 752–767.

Raghothama K. 1999. Phosphate acquisition. Annual Review of Plant Biology **50**, 665–693.

Rouached H, Arpat AB, Poirier Y. 2010. Regulation of phosphate starvation responses in plants: signaling players and cross-talks. Molecular Plant **3**, 288–299.

Rubio V, Linhares F, Solano R, Martín AC, Iglesias J, Leyva A, Paz-Ares J. 2001. A conserved MYB transcription factor involved in phosphate starvation signaling both in vascular plants and in unicellular algae. Genes & Development **15**, 2122–2133.

Sahu PP, Pandey G, Sharma N, Puranik S, Muthamilarasan M, Prasad M. 2013. Epigenetic mechanisms of plant stress responses and adaptation. Plant Cell Reports **32**, 1151–1159.

Secco D, Wang C, Arpat BA, Wang Z, Poirier Y, Tyerman SD, Wu P, Shou H, Whelan J. 2012. The emerging importance of the SPX domain-containing proteins in phosphate homeostasis. New Phytologist **193**, 842–851.

Secco D, Whelan J, Rouached H, Lister R. 2017. Nutrient stress-induced chromatin changes in plants. Current Opinion in Plant Biology **39**, 1–7.

Servet C, Conde e Silva N, Zhou DX. 2010. Histone acetyltransferase AtGCN5/HAG1 is a versatile regulator of developmental and inducible gene expression in Arabidopsis. Molecular Plant **3**, 670–677.

Shin H, Shin HS, Chen R, Harrison MJ. 2006. Loss of At4 function impacts phosphate distribution between the roots and the shoots during phosphate starvation. The Plant Journal **45**, 712–726.

Sims RJ 3rd, Millhouse S, Chen CF, Lewis BA, Erdjument-Bromage H, Tempst P, Manley JL, Reinberg D. 2007. Recognition of trimethylated histone H3 lysine 4 facilitates the recruitment of transcription postinitiation factors and pre-mRNA splicing. Molecular Cell **28**, 665–676.

Smith AP, Jain A, Deal RB, Nagarajan VK, Poling MD, Raghothama KG, Meagher RB. 2010. Histone H2A.Z regulates the expression of several classes of phosphate starvation response genes but not as a transcriptional activator. Plant Physiology **152**, 217–225.

Tanaka M, Kikuchi A, Kamada H. 2008. The Arabidopsis histone deacetylases HDA6 and HDA19 contribute to the repression of embryonic properties after germination. Plant Physiology **146**, 149–161.

Taverna SD, Ilin S, Rogers RS, *et al*. 2006. Yng1 PHD finger binding to H3 trimethylated at K4 promotes NuA3 HAT activity at K14 of H3 and transcription at a subset of targeted ORFs. Molecular Cell **24**, 785–796.

Tian L, Chen ZJ. 2001. Blocking histone deacetylation in Arabidopsis induces pleiotropic effects on plant gene regulation and development. Proceedings of the National Academy of Sciences, USA **98**, 200–205.

Tian T, Liu Y, Yan H, You Q, Yi X, Du Z, Xu W, Su Z. 2017. agriGO v2.0: a GO analysis toolkit for the agricultural community, 2017 update. Nucleic Acids Research **45**, W122–W129.

Ticconi CA, Abel S. 2004. Short on phosphate: plant surveillance and countermeasures. Trends in Plant Science **9**, 548–555.

Vance CP. 2001. Symbiotic nitrogen fixation and phosphorus acquisition. Plant nutrition in a world of declining renewable resources. Plant Physiology **127**, 390–397.

Vlachonasios KE, Thomashow MF, Triezenberg SJ. 2003. Disruption mutations of ADA2b and GCN5 transcriptional adaptor genes dramatically affect Arabidopsis growth, development, and gene expression. The Plant Cell **15**, 626–638.

Wang F, Deng M, Xu J, Zhu X, Mao C. 2018. Molecular mechanisms of phosphate transport and signaling in higher plants. Seminars in Cell & Developmental Biology **74**, 114–122.

Wang T, Xing J, Liu X, *et al*. 2016. Histone acetyltransferase general control non-repressed protein 5 (GCN5) affects the fatty acid composition of *Arabidopsis thaliana* seeds by acetylating fatty acid desaturase3 (FAD3). The Plant Journal **88**, 794–808.

Wang T, Xing J, Liu X, Yao Y, Hu Z, Peng H, Xin M, Zhou DX, Zhang Y, Ni Z. 2018. GCN5 contributes to stem cuticular wax biosynthesis by histone acetylation of CER3 in Arabidopsis. Journal of Experimental Botany **69**, 2911–2922.

Wu K, Malik K, Tian L, Brown D, Miki B. 2000*a*. Functional analysis of a RPD3 histone deacetylase homologue in *Arabidopsis thaliana*. Plant Molecular Biology **44**, 167–176.

Wu K, Tian L, Malik K, Brown D, Miki B. 2000*b*. Functional analysis of HD2 histone deacetylase homologues in *Arabidopsis thaliana*. The Plant Journal **22**, 19–27.

Wysocka J, Swigut T, Xiao H, *et al*. 2006. A PHD finger of NURF couples histone H3 lysine 4 trimethylation with chromatin remodelling. Nature **442**, 86–90.

Xing J, Wang T, Liu Z, *et al*. 2015. GENERAL CONTROL NONREPRESSED PROTEIN5-mediated histone acetylation of FERRIC REDUCTASE DEFECTIVE3 contributes to iron homeostasis in Arabidopsis. Plant Physiology **168**, 1309–1320.

Xu L, Zhao H, Wan R, *et al*. 2019. Identification of vacuolar phosphate efflux transporters in land plants. Nature Plants **5**, 84–94.

Yang XJ, Finnegan PM. 2010. Regulation of phosphate starvation responses in higher plants. Annals of Botany **105**, 513–526.

Ying Y, Yue W, Wang S, Li S, Wang M, Zhao Y, Wang C, Mao C, Whelan J, Shou H. 2017. Two h-type thioredoxins interact with the E2 ubiquitin conjugase PHO2 to fine-tune phosphate homeostasis in rice. Plant Physiology **173**, 812–824.

Zhang J, Mujahid H, Hou Y, Nallamilli BR, Peng Z. 2013. Plant long ncRNAs: a new frontier for gene regulatory control. American Journal of Plant Sciences **4**, 1038.

Zhang Y. 2006. It takes a PHD to interpret histone methylation. Nature Structural & Molecular Biology **13**, 572–574.

Zheng M, Liu X, Lin J, *et al*. 2018. Histone acetyltransferase GCN5 contributes to cell wall integrity and salt stress tolerance by altering expression of cellulose synthesis genes. The Plant Journal **97**, 587–602.